Chemical Science

EDGE ARTICLE

View Article Online
View Journal | View Issue

Cite this: *Chem. Sci.*, 2015, **6**, 486

"Self-repairing" nanoshell for cell protection†

Nan Jiang,[a] Xiao-Yu Yang,*[a] Guo-Liang Ying,[c] Ling Shen,[a] Jing Liu,[a] Wei Geng,[a] Ling-Jun Dai,[a] Shao-Yin Liu,[a] Jian Cao,[d] Ge Tian,[a] Tao-Lei Sun,[a] Shi-Pu Li[a] and Bao-Lian Su*[ab]

Received 29th August 2014
Accepted 17th October 2014

DOI: 10.1039/c4sc02638a

www.rsc.org/chemicalscience

Self-repair is nature's way of protecting living organisms. However, most single cells are inherently less capable of self-repairing, which greatly limits their wide applications. Here, we present a self-assembly approach to create a nanoshell around the cell surface using nanoporous biohybrid aggregates. The biohybrid shells present self-repairing behaviour, resulting in high activity and extended viability of the encapsulated cells (eukaryotic and prokaryotic cells) in harsh micro-environments, such as under UV radiation, natural toxin invasion, high-light radiation and abrupt pH-value changes. Furthermore, an interaction mechanism is proposed and studied, which is successful to guide design and synthesis of self-repairing biohybrid shells using different bioactive molecules.

Introduction

Self-repair is a common and wonderful phenomenon of living organisms to allow them to adapt to constantly changing environments through long term evolution.[1] However, it is rarely seen in single cells, which might be a result of evolution of unicellular organisms to multicellular organisms having more advanced environmental adaption and self-protection capability. It is therefore of great interest to endow the single cell with self-repair behaviour. A cell-in-shell structure without complicated genetic manipulation is currently regarded as the most efficient non-biogenic route to cell protection and functionalization.[2–12] The nanostructured shell materials with tunable physico-chemical properties provide an indispensible platform to endow cells with new functionalities,[13–25] such as magnetic cell-in-Fe_3O_4 shell,[15,16] thermally durable cell-in-SiO_2 shell[17] and cell-in-SiO_2/TiO_2 shell,[18] electrically conductive cell-in-Au/Ca/graphene shell,[19] UV-resistant cell-in-$LnPO_4$ shell[20] and pH-responsive cell-in-poly(methacrylic acid)-co-NH_2 shell.[21] However, traditional nanostructured shells do not satisfy the increasing demands of modern applications because these synthetic shells not only disturb cell proliferation and life cycle, but also are unable to re-assemble onto the cell surface after the process of encapsulation.[26] Once shell structures are broken, which is often caused by cell division, the decrease of stability and loss of functionalities of encapsulated cells and/or daughter cells will occur.[27] A path to self-repair of the functional nano-scale shell is mostly preferred, whereby the preformed precursor could self-assemble onto the cell surface during cell division.

Natural amino acids can non-covalently bind with the cell surface due to their bioactive groups (*e.g.* amino group, carboxyl group and/or thiol group *etc.*). They could, therefore, readily self-assemble onto the cell surface to form a nanothin meso-scaled layer. Also as the most basic biomolecules that do not require complicated synthetic procedure, amino acids possess similar physico-chemical properties to small biomolecules of cell, and therefore can be good candidates to form nanoshells. However, amino acid molecules alone may be transported through cell membrane/walls, suggesting that the amino acid molecules are not stable onto the cell surface as shell materials.[28] As is known, amino acid molecules can interact with gold nanoparticles which have been successfully introduced to shell materials.[29–31] In this study, biohybrid aggregates composed of Au nanoparticles and L-cysteine molecules have been successfully developed to fabricate the nanoshell around the cell surface and endow the encapsulated cell with the self-repairing property. This self-assembled Au@L-cysteine biohybrid nanothin shell presents a worm-like porous structure due to the properties and nano-effect of Au nanoparticles. Interestingly, the nanoporous biohybrid shell would not only allow fast mass exchange, and increase cell activity and stability in synthetic environments, but also offer the encapsulated cells more functionalities to expand their applicability, such as protecting the cells against strong UV radiation, natural toxins, high light radiation, and abrupt pH changes. Most importantly,

[a]*State Key Laboratory of Advanced Technology for Materials Synthesis and Processing, School of Materials Science and Engineering, Wuhan University of Technology, 430070 Wuhan, China. E-mail: xyyang@whut.edu.cn; tian.ge@yahoo.com; baoliansu@whut.edu.cn*

[b]*Laboratory of Inorganic Materials Chemistry, The University of Namur (FUNDP), B-5000 Namur, Belgium. E-mail: bao-lian.su@fundp.ac.be*

[c]*School of Material Science and Engineering, Wuhan Institute of Technology, 430073 Wuhan, China*

[d]*Department of Chemistry and Biochemistry, University of California San Diego, La Jolla, CA 92037, USA. E-mail: jiancaoucsd@gmail.com*

† Electronic supplementary information (ESI) available. See DOI: 10.1039/c4sc02638a

the self-assembled Au@L-cysteine hybrid aggregates dispersed in the culture solution can act as sol precursors to self-repair broken shells and form integrated shells.

The formation of the biohybrid aggregates was first investigated. L-cysteine was added to an Au colloid (2–3 nm in diameter from the transmission electron microscopy (TEM) micrograph in Fig. S1a†) at room temperature. Precipitates were characterized after collection by centrifugation–washing steps. The TEM micrograph depicts that the biohybrid aggregates present nanoporous structure with 4–8 nm pore size (Fig. S1b†). The Fourier transform infrared spectroscopy (FTIR) and the X-ray photoelectron spectroscopy (XPS) spectra confirm the formation of Au–S bonds (Fig. S2a and b†),[32,33] indicating that the interaction and structure of biohybrids are stable. The UV-vis spectrum shows that the Au@L-cysteine biohybrids not only can absorb excess high light (Fig. S2c†), but are also stable in solution (Fig. S2d†). It is safe to conclude that the nanosized Au@L-cysteine biohybrids are stable in solution and present a nanoporous structure. These properties not only enable self-assembly and self-repairing of shells, but also facilitates mass communication.

Yeast cells *Saccharomyces cerevisiae* have been selected as our model eukaryotic cells to study self-repairing behaviours. In a typical preparation of self-repairing yeast cell-in-shell structures (Fig. S1†), the biohybrid aggregates are firstly dispersed in phosphate buffer solution (PBS). Subsequently, the aggregates are added to the clean cell solution under gentle shaking at room temperature. During the interaction between the native yeast cells (Fig. S1c†) and the preformed precursors, native cells are gradually entrapped in the biohybrid shell formed by the condensation of the meso-structured Au@L-cysteine aggregates (Fig. S1d†). The entrapped cells and excess biohybrid aggregates are collected and re-dispersed into fresh medium for further incubation under ambient conditions. SEM (scanning electron microscopy), OM (optical microscopy) and TEM micrographs (Fig. 1) clearly depict that the yeast cells are individually and separately entrapped in dense shells and maintain their original morphologies, which strongly argues that such a self-assembly has no negative effect on the biological morphologies of the cells. Biohybrid aggregates on the cell surface form a worm-like nanoporous structure (inset in Fig. 1b), and the nanopore size is 2–6 nm, which is slightly smaller than the TEM data of preformed precursors (Fig. S1b†). Probably a little deformation of nanochannels occurs due to the interaction between the soft structured biohybrid aggregates and cell surface. The microtome-sliced TEM micrograph (Fig. 1c) shows that the cell is entrapped in the uniformly nanothin shell with 160 nm of thickness, and cell integrity is maintained. The EDX line profile of cell@biohybrid shell confirms that biohybrid aggregates containing Au element are uniformly coated on the cell surface (Fig. 1d and inset). Furthermore, cell culture experiments show that the growth curve of encapsulated cells is similar to that of native cells, which indicates that the nanoshell has no obvious effect on cell division (Fig. S3†). All together it can be concluded that (1) our procedure is facile and does not need numerous cycles of multilayer deposition in comparison with traditional layer-by-layer methods, meaning that cell activity could be well maintained after encapsulation; (2) the biocompatible biohybrid aggregates can effectively and easily coat onto the cell surface by self-assembly, which is beneficial for self-repair when the shell is broken; (3) nanothin and nanoporous structures of shells have been developed which would facilitate mass and energy transportation and cell division.

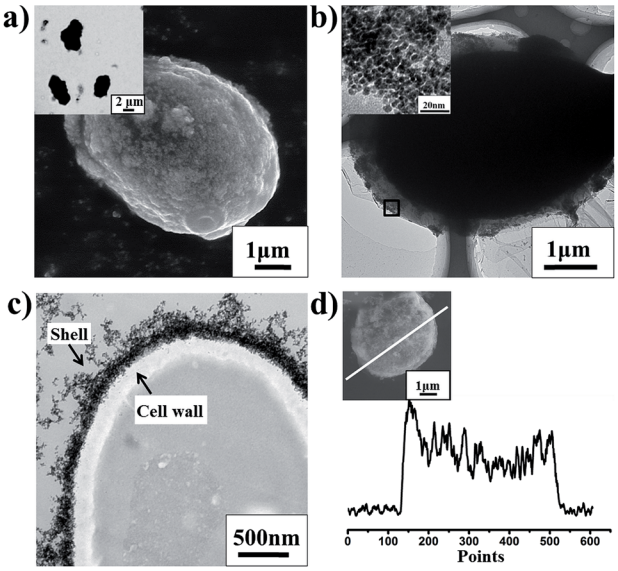

Fig. 1 Characterization of yeast cell-in-shell structure. (a) SEM and OM in a visible light mode (inset) micrographs of yeast cells@biohybrid shells; (b) TEM micrographs of yeast@biohybrid shell and the corresponding magnified micrograph of black square area (inset) show that the single cell is coated with nanoporous-structured biohybrid shell; (c) ultrathin section TEM micrograph of yeast@biohybrid shell; (d) EDX line profile for Au encapsulated yeast cells confirms the presence of biohybrid shells.

Results and discussion

To test whether the biohybrid shells protect cells in harsh conditions during cell proliferation, relative activities of encapsulated yeast cells have been carried out with native yeast cells as a comparison. It has been proven that cells keep their ability to proliferate in fresh media (Fig. S4†). Therefore, the encapsulated yeast cells are cultivated in fresh liquid media and in normal solution (without fresh medium) under short wave ultraviolet radiation (UVC, strongest ultraviolet band of sunlight for destroying genetic structure of cells[34]) (Fig. 2). Encapsulated yeast cells maintain higher activity under UVC radiation. For example, even after 5 hours radiation, 98% (±6%) of the initial activity of encapsulated cells in fresh medium remain (Fig. 2a), while native cells in medium (Fig. 2c) quickly lose their activity within 5 hours. When in normal solution without medium, yeast cell@biohybrid shell (Fig. 2b) also shows higher activity than yeast cell within silica (Fig. S5†) and native yeast cells (Fig. 2d) in normal solution. Their lower activity, compared with the encapsulated cells in fresh medium, should be attributed to the cells' ability to divide being

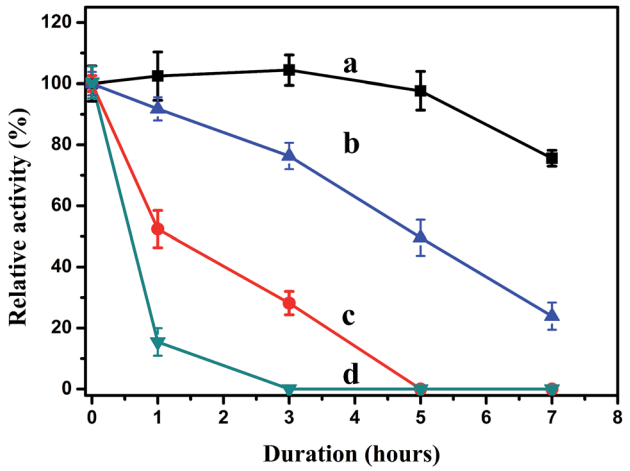

Fig. 2 Relative activities of yeast@biohybrid shell exposed under UVC radiation. Relative activities by yeast@biohybrid shell and native yeast exposed under UVC radiation in (a) and (c) fresh cultural medium, and (b) and (d) solution without cultural medium.

inhibited in the absence of the fresh medium. Furthermore, the test of nanosized natural toxin (lyticase)[35] invasion shown in Fig. S6† can also prove that the shells can protect the cells against natural toxin invasion.

It is also necessary to point out that encapsulated cells can easily break their shells during cell division since the shell is very thin and soft. That seems to easily cause loss of functionalities and a decrease in stability. However, the encapsulated yeast cells mentioned above still show high stability in proliferation. Therefore, there should be a presence of other protection mechanism. The surfaces and morphologies of the yeast cells during division are shown in the SEM micrographs in Fig. 3(a–e) and Fig. S7A.† The micrographs show that the generation of a yeast cell is typical budding reproduction, and the morphologies of cells during the budding are normal and do not shrink. Notably, nanoparticles aggregated on the cell surfaces do not show significant decreases in the 5 stages of the life cycle (G0, S, G2, M and G1 phases, see Fig. 3 and Fig. S7A†). The shell thickness of the dividing cell (around 140 nm, Fig. 3f) becomes slightly thinner, compared with that of the single cell (around 160 nm, Fig. 1C) because the enlarged surface area during cell division will make the shell become thinner. It is surely impossible to cover both mother cell and daughter cell only by the original biohybrid shell, despite the shells being soft and allowing deformation. The excess biohybrid aggregates could play an important role in self-assembly onto the naked buds and/or daughter cells because the only possibility is that the excess biohybrid aggregates in solution self-repair the thinner shells and/or broken shells.

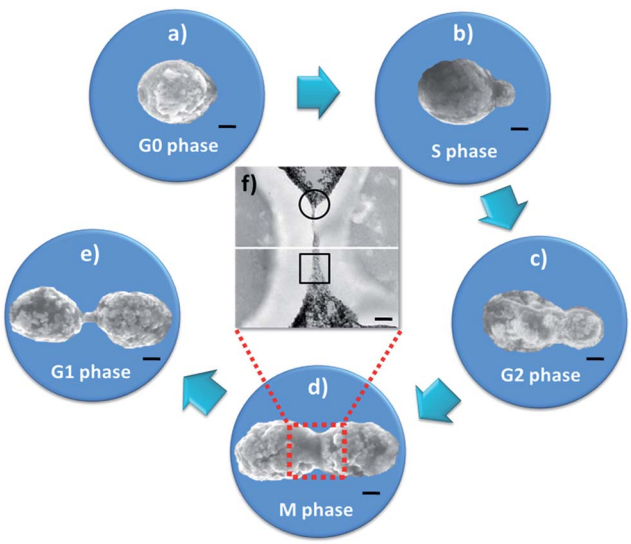

Fig. 3 Process of self-repairing biohybrid nanoshells in yeast cell division (a–e), (scale bar: 1 μm). (a) Encapsulated mother yeast cell (G0 phase); (b) encapsulated mother cell and bud (S phase); (c) encapsulated mother cell and growing bud (G2 phase); (d) encapsulated mother cell and bud of the same size as the mother cell (M phase); (e) encapsulated mother and daughter cells (G1 phase). (f) Merged magnified ultrathin section TEM micrograph of encapsulated dividing cell (scale bar: 250 nm). All original details are shown in Fig. S7.†

Direct evidence of self-repair is observed in the marked square and circle areas in Fig. 3f and Fig. S7B.† There is no difference in shell thickness between the mother cell and the bud (circle area in Fig. S7B (b)†). This means that the biohybrid aggregates can self-assemble onto the naked surfaces of both the mother cell and the bud. More interestingly, biohybrid aggregates have been found in the newly generated interface between mother cell and the bud (square area in Fig. S7B(a)†). This suggests that the generated interface is subsequently filled by original biohybrid shell aggregates or excessive nano-aggregates after cell division. It is a unique phenomenon, where it seems that the broken shell can be self-repaired by self-assembled biohybrid aggregates, and also an excellent advantage, indicating that cells are protected and functionalized by biohybrid shells in the life cycle. In contrast, the self-assembling phenomenon can hardly be found in yeast cell@polymer matter (Fig. S8a and b†) and cells within inorganic matter (Fig. S8c and d†) in the presence of excess shell materials. The results confirm that traditional polymeric or inorganic shells are not self-repair, even in the presence of excess shell precursors, directly attributed to easily polymerization of the traditional bulky polymeric precursors during the cell encapsulation procedure. The aggregation behaviours of typical polymeric nanocomposites are also evidenced (Fig. S9a and b†). TEM images clearly evidence that Au@PAH (poly allyamine hydrochloride) (Fig. S9a†) and Au@PLL (poly L-lysine) (Fig. S9b†) nanocomposites are easily polymerized to very large particle aggregates or large scale net-like aggregates. As is well known, these large aggregates or precipitates are difficult to self-assemble onto the cell surface or self-repair the broken shell. In contrast, small amino acid molecule-based nano-aggregates (Au@L-cysteine biohybrids) (Fig. S9c†) could easily achieve the goal of self-repairing property due to the nano-effect and their surface bound functional groups. This is a big advantage of small amino acid molecules in the self-repairing of shells.

Such a self-repairing phenomenon is not only limited to eukaryotic cells. It could also be extended to prokaryotic cell

systems. Cyanobacteria, which play a major role in the global carbon cycle,[36] have been picked as a typical example of prokaryotic cells. The self-repairing process of encapsulated cyanobacteria is also observed by SEM and TEM images (Fig. 4A and B). Fig. 4A shows that the reproduction of cyanobacteria is a typical binary fission, and morphologies of cells are normal and do not shrink, implying that the shells do not limit the encapsulated cells' division. The nanoparticles are clearly observed to aggregate on cell surfaces in the whole division cycle. Compared with yeast cells, the shells of the encapsulated cyanobacteria cells show a thinner thickness (around 100 nm, Fig. 4B). This indicates that the interaction between the biohybrid aggregates and the cyanobacterium is possible weaker than the yeast cell, attributed to the different bio- and physicochemical properties of the cells' surfaces. Furthermore, the self-repairing biohybrid shell could also act as a safeguard to protect cyanobacteria from harsh conditions, such as high light and strong UV radiation, and abrupt pH changes (Fig. S10†).

All the protection to UVC and high-light radiation, natural toxin invasion and abrupt pH change should be attributed to the biohybrid shell, for example, the strong absorption of UVC and high-light (in wavelength of 190–280 nm (Fig. S11†), and 450–700 nm (Fig.S2d)), strong interaction between the amino acid and nature toxin (Table S1†), and good buffering capacity of amino acid molecules. It is notable that the cell protection during proliferation would be due to the self-repairing behaviour of the encapsulated cells. Self-assembly between nano-aggregates and cell surface is the critical factor of this self-repair. It is reasonable to consider self-repairing behaviours caused by self-assembly. We cultivated yeast cells in biohybrid solution (Fig. 5a) and on a biohybrid-coated silicon substrate (Fig. 5b), respectively. SEM images clearly show that with the time being prolonged, the biohybrid aggregates on cell surfaces gradually increase from a loose structure to a dense structure under both sets of conditions. There is no obvious difference in the cell surface after 10 hours compared with that after 8 hours in the case of the cells in the biohybrid solution (Fig. S12†), indicating that the thickness of shell cannot increase unlimitedly with time being prolonged. Similarly, in the case of the cells on the biohybrid coated silicon substrate, the shell grows uniformly from bottom to top. These results point to a clear demonstration that the biohybrid aggregates could actively self-assemble onto a cell surface to form a dense shell, even by cultivating the cells on a biohybrid coated silicon substrate, which is the direct reason why the nano-aggregates can self-repair the shells.

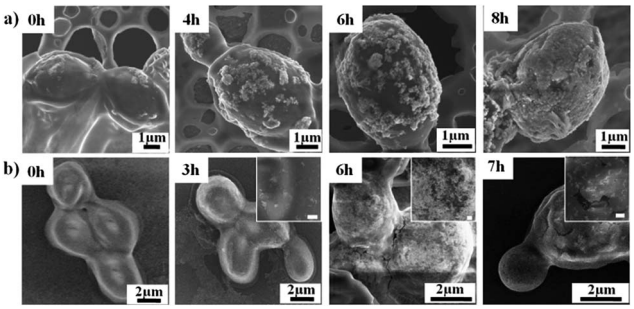

Fig. 5 SEM images of yeast cells (a) in biohybrid solution, and (b) on silicon substrate surfaces coated by biohybrid aggregates for various times. Insets are magnified images, scale bar: 200 nm.

The formation of a uniform nanoshell and shell thickness are possibly related to the surface charges and potentials of cells and biohybrids. Surface charges and potentials of cells and biohybrids have been measured by zeta potentials (ζ), where ζ(yeast cell) is -17.1 ± 1.2 mV, ζ(cyanobacteria) is -14.2 ± 0.8 mV, ζ(biohybrid) is -19.3 ± 0.7 mV (Table S2†). After encapsulation, zeta potentials of encapsulated cells are higher than native cells (ζ(yeast cell@biohybrid shell) is -18.5 ± 1.5 mV, ζ(cyanobacteria@biohybrid shell) is -16.4 ± 1.4 mV) (Table S2†). This means that the encapsulated cells provide better dispersion than native cells because the charged encapsulated cells repel one another and therefore overcome the natural tendency of cells to aggregate.[37] According to the simplified Grahame equation for low zeta potential ($\sigma = \varepsilon\varepsilon_0\zeta/\lambda_D$, where ε is dielectric permittivity and λ_D is the Debye length),[38] surface charge (σ) is positive proportional to zeta potential. In our proposed model, the negatively charged cell surfaces are possibly attracted electrostatically to the ion pair (negatively charged biohybrid aggregates with cationic ions (M^+)) forming an electrical triple layer (Fig. 6a).[39,40] After self-assembling onto the cell surface, the biohybrid aggregates intimately coat the cell surface *via* hydrogen-bonds between amino groups/carboxyl groups of the cysteine molecules in the biohybrid aggregates and the functional groups (such as amino groups and carboxyl groups of proteins and hydroxyl groups of polysaccharide) of the cell surface (Fig. 6b). It is evidenced that pure cysteine molecules can also form a net-like aggregation on the cell surface (Fig. S13a,† the smooth native cell surface is the comparison in Fig. S13b†), in spite of its instability. These interactions might cause the deformation of nanopores of nanoaggregates, corresponding with the previous results shown in Fig. 1b and S1b.† After encapsulation, moreover, yeast cells can attract more charged biohybrid aggregates due to their higher surface charge, compared with cyanobacteria surface, which gives a reason for the biohybrid shell on yeast cell surfaces being thicker than the shell on cyanobacteria surfaces.

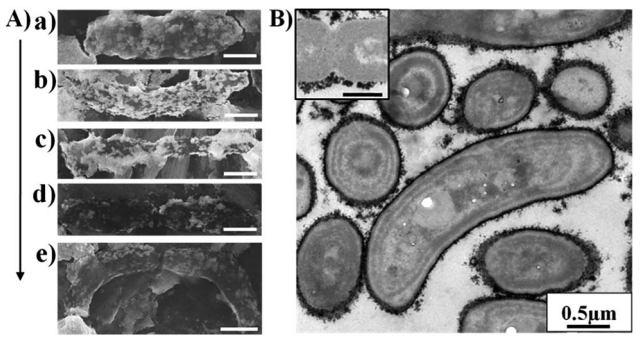

Fig. 4 (A) Process of self-repairing biohybrid nanoshell in cyanobacteria division (a–e); (B) microtome-sliced TEM micrograph and magnified micrograph (inset) of encapsulated cyanobacteria (scale bar: 0.5 μm).

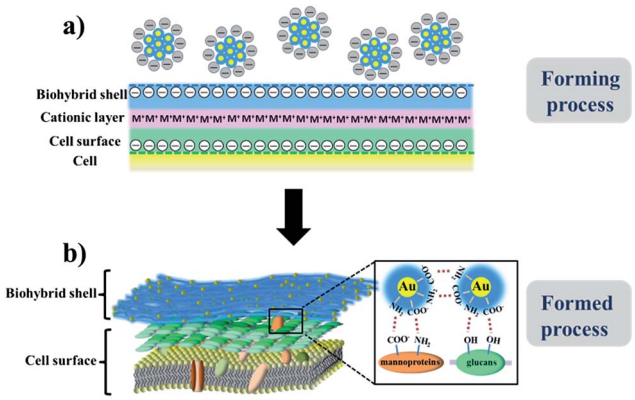

Fig. 6 Formation mechanism of self-repairing biohybrid shell on yeast cell surface. (a) Ionic interactions proposed between cell and nano-aggregates during forming process, where M^+ is cationic ions in solution; (b) interaction between the cell surface and biohybrid shell after formation.

This is also in very good agreement with the TEM results (Fig. 1c and 4B). With the increased thickness of shell, the surface charge of encapsulated cells would reach a balance where the biohybrid aggregates in solutions could not continue to assemble onto the original biohybrid shell (Fig. 6a). When the shell is broken during the cell proliferation, this balance is broken and the encapsulated yeast cell would absorb and re-assemble the nano-aggregates to self-repair the shell. Such a self-repairing behaviour is analogous to a certain self-repairing method in living organisms, where the broken area is self-repaired by the uptake of external precursors. For example, diatoms absorb silicon sources from their living environment to re-build their silica shell during cell division.[41,42] These proposed models are in good agreement with the experimental results, which are helpful to understand the self-repairing behaviour of encapsulated cells.

Furthermore, in our case, negative charges encapsulated around the cells do not affect the intrinsic characteristics of cell surface charge,[43] which avoid cell surface damage caused by traditional positively charged polyelectrolyte shell.[44] Different bioactive molecules can be therefore easily introduced to form self-repairing biohybrid shells, such as different amino acids and peptides. These shells can also be engineered onto the cell surface to protect cells. For example, cyanobacteria within Au@L-lysine hybrid shells show higher photosynthetic activity under high light radiation (Fig. S14a†). Cyanobacteria cells within Au@glutathione shells have been clearly confirmed by the microtome-sliced TEM image (Fig. S14b†).

Conclusions

To conclude, we have described an experimental success of the use of biohybrid nanoshells in cell-in-shell encapsulation to endow the encapsulated cells with self-repairing behaviour. These self-repairing shells present structural superiority of nanopores and nanolayers, and provide the cells with excellent protection. The interaction mechanism has been investigated in detail, and guided the synthesis of the self-repairing biohybrid shells using different bioactive molecules. It is believed that our strategy is not limited to yeast and cyanobacteria, and should be applicable to higher eukaryotes, such as human cells, even multicellular organisms.[25] Furthermore, other functional matter can also be used to enhance cell activity and introduce various functionalities. For example, bioactive proteins can be used to improve the selective activity; polymers can be used to design smart interfaces; oxides can be used to introduce magnetic, electronic, optical, and thermal properties. The self-repairing strategy developed here therefore offers a general, facile, and unique approach for the encapsulation of cells with long-term viability, extraordinary stability, high activity and multiple functionalization.

Acknowledgements

This work was supported by the Chinese Ministry of Education (NCET-11-0688, IRT1169, RFDP-20110143120006, 2012-YB-04), NFSC-51101115, NFSC-51472190. B.L.S. acknowledges "Program of Global Expert" and program of "Chang Jiang Scholar". X.Y.Y. acknowledges the program of "Chutian Scholar". N.J. carried out all the experiments. X.Y.Y. conceived the project, provided the idea, and designed and guided the experiments. G.T. guided the synthesis of the precursor. G.L.Y., W.G. and G.T. analysed the data and edited the figures. L.S., L.J.D., S.Y.L. carried out precursor preparation. J.L. performed the TEM measurements. T.L.S. and S.P.L. analysed the data and support guidance of interface materials. B.L.S. conceived the project, and supported scientific and technological platform and guidance. N.J. and X.Y.Y. wrote and revised the paper. J.C. and B.L.S. revised the paper.

Notes and references

1 J. F. Miller, *Genetic and Evolutionary Computation–GECCO 2004*, Springer, Berlin Heidelberg, 2004, p. 129.
2 I. Drachuk, M. K. Gupta and V. V. Tsukruk, *Adv. Funct. Mater.*, 2013, **23**, 4437.
3 E. C. Carnes, D. M. Lopez, N. P. Donegan, A. Cheung, H. Gresham, G. S. Timmins and C. J. Brinker, *Nat. Chem. Biol.*, 2010, **6**, 41.
4 N. Nassif, O. Bouvet, M. N. Rager, C. Roux, T. Coradin and J. Livage, *Nat. Mater.*, 2002, **1**, 42.
5 R. F. Fakhrullin and Y. M. Lvov, *ACS Nano*, 2012, **6**, 4557.
6 R. F. Fakhrullin, A. I. Zamaleeva, M. V. Morozov, D. I. Tazetdinova, F. K. Alimova, A. K. Hilmutdinov, R. I. Zhdanov, M. Kahraman and M. Culha, *Langmuir*, 2009, **25**, 4628.
7 V. Kozlovskaya, S. Harbaugh, I. Drachuk, O. Shchepelina, N. Kelley-Loughnane, M. Stone and V. V. Tsukruk, *Soft Matter*, 2011, **7**, 2364.
8 S. H. Yang, S. M. Kang, K.-B. Lee, T. D. Chung, H. Lee and I. S. Choi, *J. Am. Chem. Soc.*, 2011, **133**, 2795.
9 A. I. Zamaleeva, I. R. Sharipova, A. V. Porfireva, G. A. Evtugyn and R. F. Fakhrullin, *Langmuir*, 2010, **26**, 2671.

10 S. R. Shin, H. Bae, J. M. Cha, J. Y. Mun, Y.-C. Chen, H. Tekin, H. Shin, S. Farshchi, M. R. Dokmeci, S. Tang and A. Khademhosseini, *ACS Nano*, 2012, **6**, 362.
11 R. F. Fakhrullin and R. T. Minullina, *Langmuir*, 2009, **25**, 6617.
12 J. Lee, S. H. Yang, S.-P. Hong, D. Hong, H. Lee, H.-Y. Lee, Y.-G. Kim and I. S. Choi, *Macromol. Rapid Commun.*, 2013, **34**, 1351.
13 H. Ai, M. Fang, S. A. Jones and Y. M. Lvov, *Biomacromolecules*, 2002, **3**, 560.
14 S. S. Balkundi, N. G. Veerabadran, D. M. Eby, G. R. Johnson and Y. M. Lvov, *Langmuir*, 2009, **25**, 14011.
15 R. F. Fakhrullin, J. García-Alonso and V. N. Paunov, *Soft Matter*, 2010, **6**, 391.
16 S. Y. Yang, T. Lee, E. Seo, E. H. Ko, I. S. Choi and B.-S. Kim, *Macromol. Biosci.*, 2012, **12**, 61.
17 G. C. Wang, L. J. Wang, P. Liu, Y. Yan, X. R. Xu and R. K. Tang, *ChemBioChem*, 2010, **11**, 2368.
18 J. Lee, J. Choi, J. H. Park, M.-H. Kim, D. Hong, H. Cho, S. H. Yang and I. S. Choi, *Angew. Chem., Int. Ed.*, 2014, **53**, 8056.
19 R. Kempaiah, S. Salgado, W. L. Chung and V. Maheshwari, *Chem. Commun.*, 2011, **47**, 11480.
20 B. Wang, P. Liu, Y. Y. Tang, H. H. Pan, X. R. Xu and R. K. Tang, *PloS One*, 2010, **5**, e9963.
21 I. Drachuk, O. Shchepelina, M. Lisunova, S. Harbaugh, N. Kelley-Loughnane, M. Stone and V. V. Tsukruk, *ACS Nano*, 2012, **6**, 4266.
22 X. Y. Yang, G. Tian, N. Jiang and B. L. Su, *Energy Environ. Sci.*, 2012, **5**, 5540.
23 W. Xiong, Z. Yang, H. L. Zhai, G. C. Wang, X. R. Xu, W. M. Ma and R. K. Tang, *Chem. Commun.*, 2013, **49**, 7525.
24 J. T. Wilson, W. X. Cui and E. L. Chaikof, *Nano Lett.*, 2008, **8**, 1940.
25 R. T. Minullina, Y. N. Osin, D. G. Ishmuchametova and R. F. Fakhrullin, *Langmuir*, 2011, **27**, 7708.
26 A. Diaspro, D. Silvano, S. Krol, O. Cavalleri and A. Gliozzi, *Langmuir*, 2002, **18**, 5047.
27 S. Krol, A. Diaspro, R. Magrassi, P. Ballario, B. Grimaldi, P. Filetici, P. Ornaghi, P. Ramoino and A. Gliozzi, *IEEE Transactions on Nanobioscience*, 2004, **3**, 32.
28 A. Meister, *Science*, 1973, **180**, 33.
29 V. Berry and R. F. Saraf, *Angew. Chem.*, 2005, **117**, 6826.
30 V. Berry, S. Rangaswamy and R. F. Saraf, *Nano Lett.*, 2004, **4**, 939.
31 V. Maheshwari, D. E. Fomenko, G. Singh and R. F. Saraf, *Langmuir*, 2010, **26**, 371.
32 M. Koneswaran and R. Narayanaswamy, *Sens. Actuators, B*, 2009, **139**, 104.
33 K. Uvdal, P. BodÖ and B. Liedberg, *J. Colloid Interface Sci.*, 1992, **149**, 162.
34 S. G. Nair and G. R. Loppnow, *Photochem. Photobiol.*, 2013, **89**, 884.
35 J. H. Scott and R. Schekman, *J. Bacteriol.*, 1980, **142**, 414.
36 R. Iturriaga and B. G. Mitchell, *Mar. Ecol.: Prog. Ser.*, 1986, **28**, 291.
37 B. Heurtault, P. Saulnier, B. Pech, J.-E. Proust and J.-P. Benoit, *Biomaterials*, 2003, **24**, 4283.
38 H. J. Butt, K. Graf and M. Kappl, *Physics and chemistry of interfaces*. John Wiley & Sons, 2006.
39 P. Behrens, *Angew. Chem., Int. Ed.*, 1996, **35**, 515.
40 Q. S. Huo, D. I. Margolese, U. Ciesla, D. G. Demuth, P. Y. Feng, T. E. Gier, P. Sieger, A. Firouzi and B. F. Chmelka, *Chem. Mater.*, 1994, **6**, 1176.
41 E. Paasche, *Mar. Biol.*, 1973, **19**, 17.
42 V. Martin-Jézéquel, M. Hildebrand and M. A. Brzezinski, *J. Phycol.*, 2000, **36**, 821.
43 A. A. Eddy and A. D. Rudin, *Proc. R. Soc. London, Ser. B*, 1958, **148**, 419.
44 D. Fischer, Y. X. Li, B. Ahlemeyer, J. Krieglstein and T. Kissel, *Biomaterials*, 2003, **24**, 1121.